

miR-511-3p Modulates Genetic Programs of Tumor-Associated Macrophages

Mario Leonardo Squadrito,^{1,3} Ferdinando Pucci,^{1,3} Laura Magri,^{2,3} Davide Moi,¹ Gregor D. Gilfillan,⁴ Anna Ranghetti,¹ Andrea Casazza,⁵ Massimiliano Mazzone,⁵ Robert Lyle,⁴ Luigi Naldini,^{1,3} and Michele De Palma^{1,6,*}

¹Angiogenesis and Tumor Targeting Unit, and HSR-TIGET, Division of Regenerative Medicine

²Neural Stem Cell Biology Unit, Division of Regenerative Medicine
San Raffaele Institute, 20132-Milan, Italy

³Vita-Salute San Raffaele University, 20132-Milan, Italy

⁴Department of Medical Genetics and Norwegian High-Throughput Sequencing Centre (NSC), Oslo University Hospital,
Kirkeveien 166, 0407-Oslo, Norway

⁵Laboratory of Molecular Oncology and Angiogenesis, Vesalius Research Center, VIB and K.U. Leuven, 3000 Leuven, Belgium

⁶Present address: The Swiss Institute for Experimental Cancer Research (ISREC), School of Life Sciences, Swiss Federal Institute of
Technology Lausanne (EPFL), 1015 Lausanne, Switzerland

*Correspondence: michele.depalma@epfl.ch

DOI 10.1016/j.celrep.2011.12.005

SUMMARY

Expression of the mannose receptor (MRC1/CD206) identifies macrophage subtypes, such as alternatively activated macrophages (AAMs) and M2-polarized tumor-associated macrophages (TAMs), which are endowed with tissue-remodeling, proangiogenic, and protumoral activity. However, the significance of MRC1 expression for TAM's protumoral activity is unclear. Here, we describe and characterize miR-511-3p, an intronic microRNA (miRNA) encoded by both mouse and human *MRC1* genes. By using sensitive miRNA reporter vectors, we demonstrate robust expression and bioactivity of miR-511-3p in MRC1⁺ AAMs and TAMs. Unexpectedly, enforced expression of miR-511-3p tuned down the protumoral gene signature of MRC1⁺ TAMs and inhibited tumor growth. Our findings suggest that transcriptional activation of *Mrc1* in TAMs evokes a genetic program orchestrated by miR-511-3p, which limits rather than enhances their protumoral functions. Besides uncovering a role for MRC1 as gatekeeper of TAM's protumoral genetic programs, these observations suggest that endogenous miRNAs may operate to establish thresholds for inflammatory cell activation in tumors.

INTRODUCTION

Tumor-associated macrophages (TAMs) support tumor progression in mouse models of cancer (Qian and Pollard, 2010). The protumoral functions of TAMs are thought to depend, at least in part, on their production of growth, tissue-remodeling, and immunomodulatory factors. Together, these enhance tumor cell motility and invasion, activate fibroblasts to synthesize extracellular matrix (ECM) proteins, facilitate angiogenesis, and

suppress antitumor immunity (Qian and Pollard, 2010; Squadrito and De Palma, 2011; Biswas and Mantovani, 2010; Sica and Bronte, 2007). However, TAMs comprise distinct subsets, which appear to contribute differentially to tumor progression (Qian and Pollard, 2010; Squadrito and De Palma, 2011). In the mouse, high expression of the mannose receptor (MRC1/CD206) and low expression of the integrin αX (CD11c) identify a TAM subset with enhanced proangiogenic, tissue-remodeling and protumoral activities (Pucci et al., 2009; Movahedi et al., 2010); a variable proportion of these MRC1⁺CD11c^{low} TAMs also express the angiopoietin receptor, TIE2, and have thus been termed TIE2-expressing macrophages (De Palma et al., 2005; Pucci et al., 2009; Mazzieri et al., 2011). Conversely, CD11c⁺MRC1^{low} TAMs express a proinflammatory and angiostatic phenotype, and perhaps exert antitumoral functions (Pucci et al., 2009; Movahedi et al., 2010; Rolny et al., 2011). It is still unclear whether the diverse TAM subsets identified in mouse tumor models derive from distinct circulating monocyte precursors or are induced locally in the tumor from a common precursor/progenitor cell (PC) (Squadrito and De Palma, 2011). Yet, several tumor-derived factors, including cytokines produced by infiltrating immune cells, may instruct TAMs to acquire either pro- or antitumoral functions (DeNardo et al., 2010).

MRC1 is an endocytic receptor primarily expressed by subsets of macrophages and dendritic cells (DCs); it is primarily involved in the clearance of both host and microbe-derived glycoproteins (Taylor et al., 2005). MRC1 expression is strongly upregulated by IL-4 and IL-13, and downregulated by IFN- γ (Stein et al., 1992). Notably, these cytokines are pleiotropic modulators of macrophage activation; their context-dependent expression patterns may contribute to the remarkable heterogeneity of macrophage phenotypes observed throughout tissues and tumors. Whereas IFN- γ promotes a "classic" or proinflammatory macrophage activation program, IL-4 and IL-13 fuel an "alternative" macrophage activation program, which promotes ECM remodeling, angiogenesis, tissue growth, and repair (Gordon and Martinez, 2010; Martinez et al., 2009). Based on their gene expression signature and tissue-remodeling/proangiogenic activities, MRC1⁺ TAMs resemble IL-4-stimulated

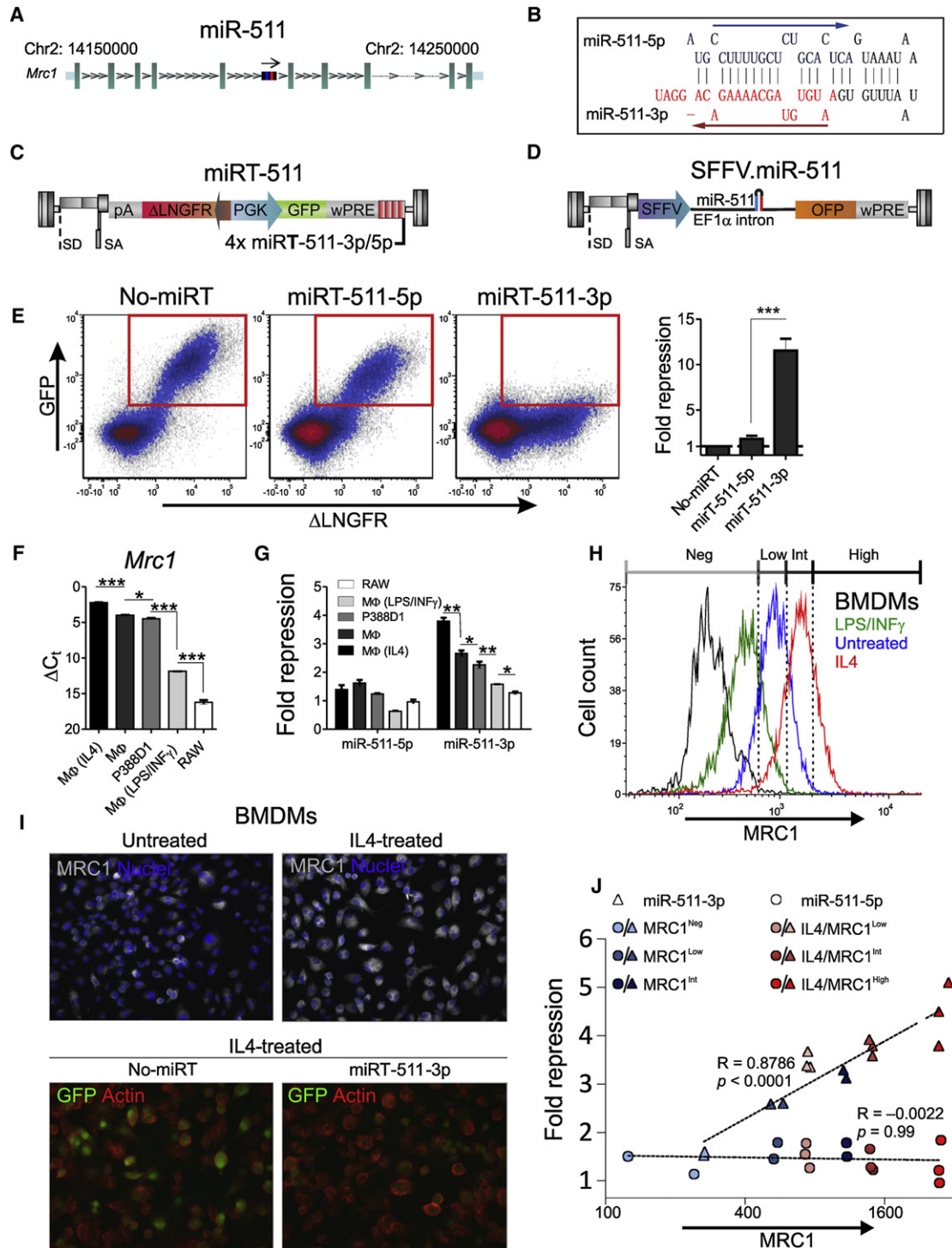


Figure 1. miR-511-3p Is the Active Strand of Mouse Pre-miR-511 and Is Coregulated with the *Mrc1* Gene

(A) Genomic region comprising the mouse miR-511 locus and the surrounding *Mrc1* gene on mouse chromosome 2, as retrieved by the UCSC (NCBI37/mm9) genome browser.

(B) Stem-loop structure of the mouse pre-miR-511. miR-511-5p and -3p sequences are shown in blue and red, respectively.

(C) Schematic of the proviral LV used to measure miR-511 activity (miRT-511 LV). The miRT sequences are cloned downstream to the GFP expression cassette, which is regulated by a bidirectional PGK promoter.

(D) Schematic of the proviral LV used to overexpress miR-511 (SFFV.miR-511 LV). The sequence of the primary miR-511 is cloned within the *EF1 α* intron, downstream to a SFFV promoter.

alternatively activated macrophages (AAMs) (Biswas and Mantovani, 2010; Gordon and Martinez, 2010). Although IL-4, IFN- γ , and several other tumor-derived cytokines and growth factors have been identified that can modulate macrophage phenotypes in vitro and in vivo (Biswas and Mantovani, 2010; DeNardo et al., 2010; Qian and Pollard, 2010), the signals in tumors that regulate pro- versus antitumoral functions of the distinct TAM subsets are still poorly defined.

MicroRNAs (miRNAs) are small, single-stranded RNAs that are generated from endogenous hairpin-shaped transcripts (called primary miRNAs). It is now well established that the unique combination of miRNAs expressed in each cell type determines the fine tuning of hundreds of mRNAs, thus regulating gene expression and cell function (Bartel, 2009). Several miRNAs have been identified that are robustly expressed by human macrophages in vitro (Tserel et al., 2011). However, to our knowledge, no information is available on the miRNA expression profiles of the distinct TAM subsets. Here, we describe and characterize an intronic miRNA, miR-511-3p, which is embedded in and coexpressed with the *Mrc1* gene. We show that the upregulation of MRC1, which is contextual with the differentiation (or alternative activation) of protumoral TAMs, triggers a negative-feedback response orchestrated by miR-511-3p that attenuates their protumoral genetic programs.

RESULTS

miR-511-3p Is the Active Strand of miR-511

We noted that the mouse *Mrc1* gene, which is primarily expressed by protumoral TAMs (Pucci et al., 2009) and AAMs (Stein et al., 1992), contains a miRNA coding sequence, miR-511 (or mmu-miR-511), located in the fifth intron of the gene (Figure 1A). Processing of the precursor miRNA (termed pre-miR-511) should generate two mature miRNAs, miR-511-5p (located at the 5' end of the pre-miRNA) and miR-511-3p (located at the 3' end of the pre-miRNA) (Figure 1B).

To investigate whether miR-511-5p and -3p are expressed and biologically active in live cells, we used a lentiviral vector (LV) reporter system for miRNA activity (Brown et al., 2007). We incorporated four miRNA target (miRT) sequences with perfect complementarity to either miR-511-5p or -3p (termed

miRT-511-5p and miRT-511-3p, respectively) into the 3' untranslated region (UTR) of a green fluorescent protein (GFP) transgene expressed from a ubiquitously active bidirectional promoter, which also controls the expression of the reporter gene, Δ LNGFR (Figure 1C). We also generated a control LV expressing a GFP sequence not containing miRT sequences in its 3' UTR (termed no-miRT). Following LV cell transduction the miRNA machinery will degrade the miRT-containing GFP transcript only in cells that express the cognate miRNA, in a manner that is dependent on miRNA abundance and/or activity. On the other hand, expression of Δ LNGFR is independent of miRNA activity and is used as an internal normalizer to calculate GFP repression by the miRNA of interest (Brown et al., 2007).

We initially studied miR-511 activity in 293T cells, which do not express miR-511 endogenously (data not shown). In order to artificially overexpress the pre-miR-511 (and thus both miR-511-5p and -3p mature miRNAs), we cloned a fragment of the *Mrc1* intron encompassing the miR-511 locus, downstream to the spleen focus-forming virus (SFFV) promoter and upstream to an orange fluorescent protein (OFP) reporter gene (Figure 1D). We termed the resultant vector SFFV.miR-511 LV. We then transduced 293T cells with the miRT-511-5p, -3p, or no-miRT reporter LVs, and superinfected the transduced cells with the SFFV.miR-511 LV. As shown in Figure 1E, overexpression of pre-miR-511 repressed GFP much more efficiently in cells transduced with the miRT-511-3p reporter LV, suggesting that the active strand of the pre-miR-511 is miR-511-3p.

The *Mrc1* Gene and miR-511-3p Are Coregulated

Intronic miRNAs can be expressed from either host gene promoters or independent transcription regulatory elements (Baskerville and Bartel, 2005; Biasiolo et al., 2011). We then asked whether expression of the *Mrc1* gene and miR-511-3p are transcriptionally coregulated. To address this question, we used mouse monocytic cell lines (RAW264.7 and P388D1; see Figure S1 available online) and bone marrow-derived macrophage (BMDM) cultures. qPCR analyses showed decreasing *Mrc1* mRNA levels in the following cell cultures: IL-4-treated BMDMs; untreated BMDMs; P388D1 cells; LPS/IFN- γ -treated BMDMs; and RAW264.7 cells (Figure 1F). These data are consistent with previous reports showing that IL-4 and LPS/IFN- γ

(E) miR-511-5p and -3p activity in 293T cells overexpressing miR-511. The cells were transduced with the miRT-511-5p, -3p, or no-miRT reporter LVs, and superinfected with the SFFV.miR-511 overexpressing LV. Dot plots show GFP and Δ LNGFR expression from the indicated reporter LVs. The histogram on the right shows quantification of GFP repression (mean values \pm SEM versus no-miRT control; n = 2 independent experiments). Statistical analysis of fold-repression values was performed by unpaired Student's t test.

(F) Expression of the *Mrc1* gene in BMDMs (M Φ ; either untreated or stimulated as indicated), P388D1 and RAW264.7 cells. Data show mean Δ C_t values \pm SEM versus β 2 m; n = 2–3 independent experiments. Statistical analysis of Δ C_t values was performed by unpaired Student's t test.

(G) Endogenous miR-511-5p and -3p activity in BMDMs (M Φ ; either untreated or stimulated as indicated), P388D1 and RAW264.7 cells. The histograms show GFP repression (mean values \pm SEM versus no-miRT control; n = 2–8 independent experiments). Statistical analysis of fold-repression values was performed by unpaired Student's t test.

(H) MRC1 protein expression in BMDMs either untreated or stimulated as indicated. The black open line is the fluorescence minus one (FMO) control for the anti-MRC1 antibody. Data are representative of two independent experiments.

(I) Endogenous miR-511-3p activity in IL-4-stimulated BMDMs. Top panels show MRC1 protein in BMDMs either untreated or stimulated by IL-4; cell nuclei were stained by DAPI. Bottom panels show GFP in IL-4-stimulated BMDMs either transduced with the no-miRT or miRT-511-3p reporter LV; the cell's actin cytoskeleton was stained by phalloidin.

(J) Correlation between GFP repression and MRC1 protein in BMDMs either untreated or stimulated with IL-4; the cells were previously transduced with the miRT-511-5p, -3p, or no-miRT reporter LVs. GFP expression was measured after fractionating the cells according to different MRC1 protein levels (Neg, negative; Low; Int, intermediate; High; see H). Statistical analysis was performed by Spearman's rank correlation test.

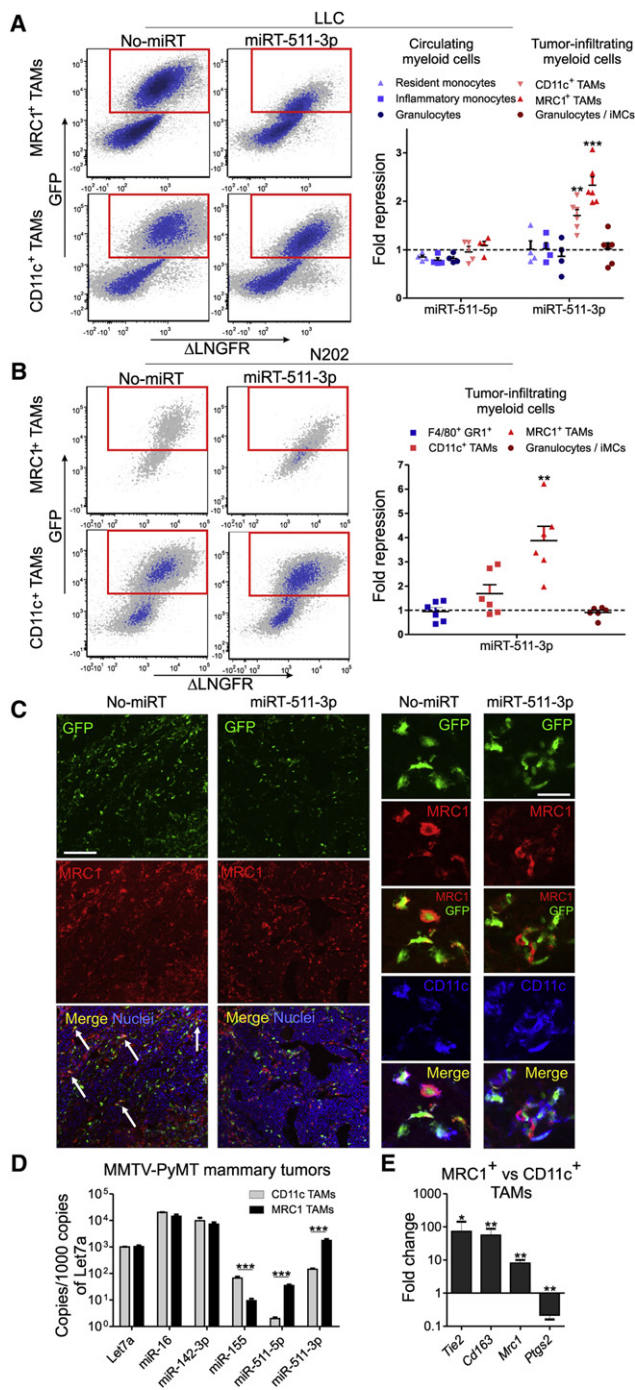


Figure 2. Preferential Expression and Activity of miR-511-3p in MRC1⁺ TAMs

(A) miR-511-3p activity in LLC grown in C57BL/6 mice. Left view shows flow cytometry analysis of GFP and Δ LNGFR in MRC1⁺ and CD11c⁺ TAMs. Right view illustrates GFP repression in the indicated cell types (versus no-miRT control). Each dot in the scatterplot corresponds to one mouse (n = 4–6/group). Statistical analysis of fold-repression values was performed by unpaired Student's t test.

(B) miR-511-3p activity in N202 mammary carcinomas grown in FVB/n mice (n = 5–6 mice/group). Statistical analysis of fold-repression values was performed by unpaired Student's t test.

robustly modulate MRC1 expression in cultured BMDMs (Stein et al., 1992). Interestingly, we found that the degree of GFP repression tightly correlated with the expression of the endogenous *Mrc1* gene in cells transduced with the miRT-511-3p but not -5p reporter LV (Figures 1F and 1G; p < 0.02 by Spearman's rank correlation test). As seen in overexpression experiments (Figure 1E), endogenous miR-511 repressed GFP much more efficiently in cells transduced with the miRT-511-3p than -5p reporter LV (Figure 1G). Finally, we found that GFP repression by miR-511-3p (but not -5p) also correlated with MRC1 protein levels (Figures 1H–1J). Together, these data corroborate the notion that miRT-511-3p is the active strand of miR-511, and strongly suggest that the *Mrc1* gene and miR-511 are transcriptionally coregulated.

Robust and Preferential Activity of miR-511-3p in MRC1⁺ TAMs

In order to analyze the expression pattern and activity of miR-511 in vivo, we implemented the aforementioned reporter system in a model of hematopoietic stem (HS)/PC transplantation. We transduced HS/PCs obtained from the BM of C57BL/6 mice with the miRT-511-5p, -3p, or no-miRT reporter LV, and transplanted the transduced cells into irradiated, syngeneic mice. Lewis lung carcinoma (LLC) cells were injected subcutaneously 4 weeks after the transplant, and the tumors were grown for an additional 4 weeks. We then measured the degree of GFP repression in a variety of circulating and tumor-infiltrating myeloid cells, including circulating “resident” and “inflammatory” monocytes, circulating granulocytes, F4/80⁺MRC1⁺CD11c^{low} and F4/80⁺CD11c⁺MRC1^{low} TAMs, and tumor-infiltrating granulocytes/immature myeloid cells (iMCs). It should be noted that the majority of TAMs are MRC1⁺ in LLCs grown in C57BL/6 mice (Figure S2A).

We did not detect GFP repression in blood cells (granulocytes, inflammatory and resident monocytes) or tumor-infiltrating granulocytes/iMCs, indicating that neither miR-511-3p nor -5p are detectably active in these cells (Figure 2A). Conversely, we detected GFP repression in MRC1⁺ and, to a lesser extent, CD11c⁺ TAMs carrying miRT-511-3p but not -5p target sequences (Figure 2A). These in vivo data confirm that miR-511-3p is the active strand of the mouse pre-miR-511, and demonstrate that endogenous miR-511-3p is preferentially active in MRC1⁺ TAMs among tumor-infiltrating and circulating myeloid cells.

(C) GFP (green), MRC1 (red), and CD11c immunostaining or nuclear staining by TO-PRO-3 (blue) of N202 mammary tumors grown in FVB/n mice. Arrows indicate GFP⁺MRC1⁺ TAMs. Scale bars, 150 μ m (left panels) and 30 μ m (RIGHT panels). Results are representative of four tumors/group.

(D) qPCR of selected miRNAs in MRC1⁺ and CD11c⁺ TAMs isolated from MMTV-PyMT mammary tumors. The data show relative abundance of each miRNA (mean values \pm SEM versus Let7a; n = 3 biological samples). Statistical analysis of Δ C_t values was performed by unpaired Student's t test.

(E) qPCR of selected mRNAs in MRC1⁺ and CD11c⁺ TAMs isolated from MMTV-PyMT mammary tumors. The data show fold change ($= 2^{\Delta\Delta C_t}$; mean values \pm SEM; n = 3 biological samples) versus CD11c⁺ TAMs (reference population). Normalization was performed by interpolating *Gapdh* and $\beta 2 m$. Statistical analysis of Δ C_t values was performed by unpaired Student's t test.

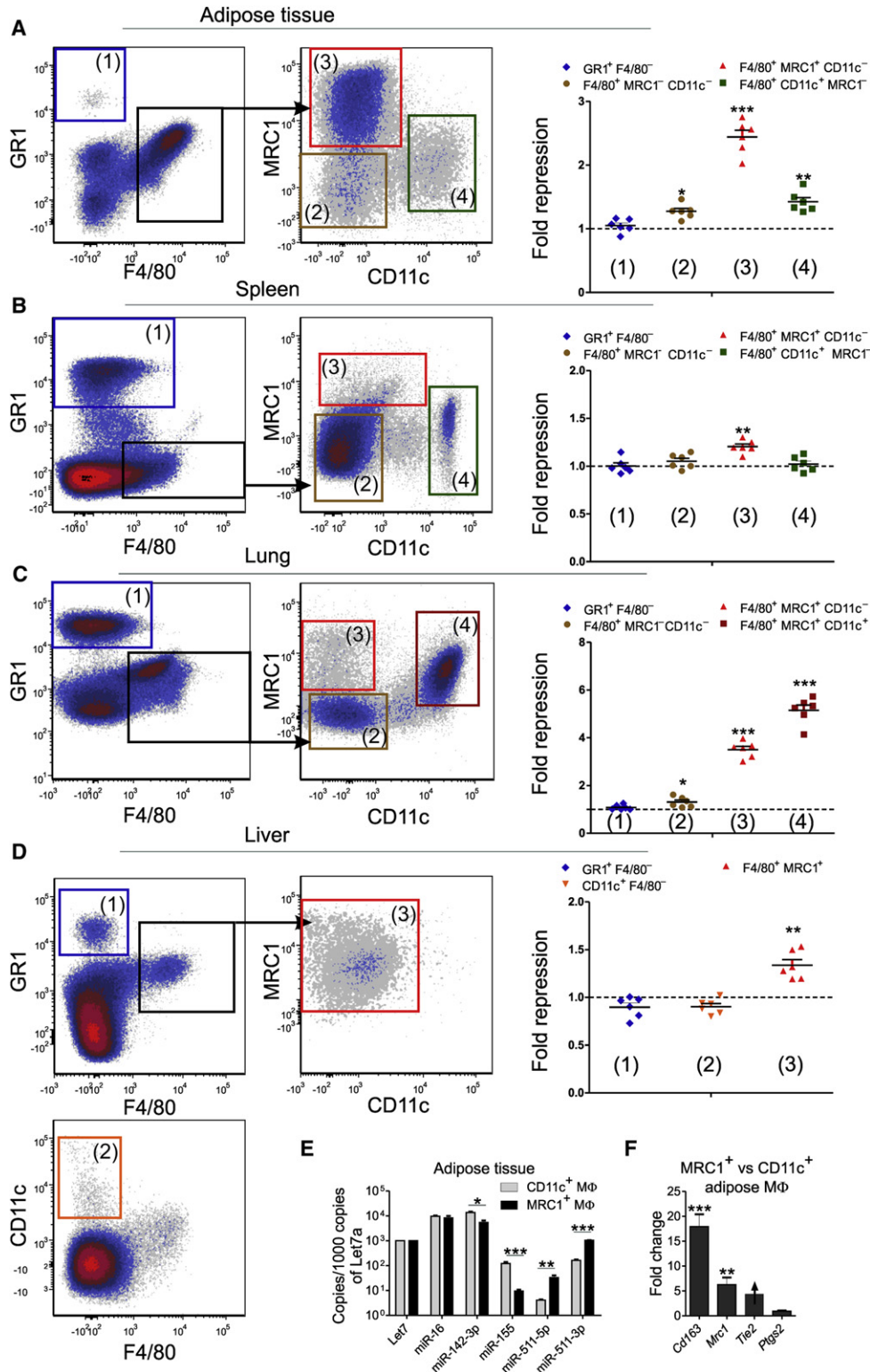


Figure 3. Preferential Expression and Activity of miR-511-3p in MRC1⁺ Tissue-Resident Macrophages

(A–D) Flow cytometry analysis of F4/80⁺ tissue-resident macrophages (further separated based on MRC1 and CD11c expression), Gr1⁺F4/80⁻ granulocytes, and CD11c⁺F4/80⁻ DCs, in the indicated tissues/organs of FVB/n mice. Flow cytometry dot plots on the left show the gating strategy. The scatterplot on the right shows GFP repression (versus no-miRT control) in the individual cell types. Each dot in the scatterplot corresponds to one mouse. Statistical analysis of fold-repression values was performed by unpaired Student's t test.

To rule out that our findings are mouse strain or tumor specific, we also analyzed miR-511-3p activity in FVB/n mice transplanted as above and challenged with N202 (Neu⁺) mammary carcinomas (Figure 2B). It should be noted that, contrary to LLCs, the majority of TAMs are CD11c⁺ in N202 tumors grown in FVB/n mice (Figure S2B). As seen in LLCs, we observed robust GFP repression (and thus miR-511-3p activity) in MRC1⁺ but not CD11c⁺ TAMs or infiltrating granulocytes/iMCs in N202 tumors analyzed at 4 weeks postinjection. These data were confirmed by immunofluorescence staining of tumor sections, showing lower GFP signal in MRC1⁺ than CD11c⁺ TAMs (Figure 2C). These findings indicate that preferential activity of miR-511-3p in MRC1⁺ TAMs is independent of the mouse strain, the tumor type, or the relative abundance of the distinct TAM subsets.

In addition to miRNA activity, we analyzed miRNA abundance by qPCR. We measured the expression of a panel of selected miRNAs, including miR-511-5p and -3p, in both MRC1⁺ and CD11c⁺ TAMs isolated from spontaneous MMTV-PyMT mammary tumors (Mazzei et al., 2011) by fluorescence-activated cell sorting (FACS). Although both miR-511-5p and -3p were significantly upregulated in MRC1⁺ versus CD11c⁺ TAMs (>10-fold), miR-511-3p levels were much higher than -5p levels in either TAM subset (Figure 2D). Of note, expression of the *Mrc1* gene was ~10-fold higher in MRC1⁺ than CD11c⁺ TAMs (Figure 2E), suggesting that in vivo as in vitro (Figures 1G and 1J) the host gene and the miRNA are transcriptionally coregulated.

miR-511-3p Is Preferentially Active in MRC1⁺ Tissue Macrophages

In addition to protumoral TAMs (Qian and Pollard, 2010; Squadrito and De Palma, 2011), certain tissue-resident macrophage populations express MRC1 (Gordon and Martinez, 2010; Martinez et al., 2009). We then asked whether miR-511-3p is also active in these cells. To this aim, we analyzed organs and tissues of FVB/n mice transplanted 8 weeks earlier with HS/PCs transduced with the miRT-511-3p or no-miRT reporter LVs (Figures 3A–3D). In agreement with the pattern of miR-511-3p activity in tumor-infiltrating myeloid cells, we detected GFP repression (and hence miR-511-3p activity) specifically in F4/80⁺Gr1[−] macrophages that express distinctly high MRC1 protein. These include MRC1⁺CD11c[−] adipose tissue macrophages (Chawla et al., 2011), MRC1⁺ lung/alveolar macrophages (Landsman and Jung, 2007), MRC1⁺CD11c[−] spleen red pulp macrophages, and MRC1⁺CD11c[−] liver Kupffer cells (Taylor et al., 2005). On the other hand, Gr1⁺F4/80[−] granulocytes, CD11c^{high}F4/80[−] DCs, and other MRC1-negative myeloid cells all displayed negligible miR-511-3p activity (Figures 3A–3D).

To corroborate these findings with miRNA expression data, we isolated macrophages from the adipose tissue by FACS, and measured the expression of a panel of selected miRNAs, including miR-511-5p and -3p. In agreement with the GFP

repression data, we observed significantly higher miR-511-3p levels in MRC1⁺CD11c[−] than CD11c⁺MRC1[−] adipose tissue macrophages (Figure 3E). As seen in TAMs (Figure 2E), miR-511-3p levels were consistently higher than -5p levels in each macrophage subset (Figure 3E). Of note, abundance of the *Mrc1* mRNA correlated with that of miR-511-3p (Figure 3F), further supporting the notion that the host gene and the miRNA are transcriptionally coregulated. Taken together, these data demonstrate robust miR-511-3p expression and activity in distinct MRC1⁺ tissue-macrophage subtypes.

ROCK2 Is a Direct Target of miR-511-3p

We then used TargetScan (Lewis et al., 2005) and DIANA microT (Maragkakis et al., 2009) to identify miR-511-3p predicted targets. The analysis retrieved a list of 145 genes (Table S1) that we analyzed by DAVID Bioinformatic resources 6.7 (Huang et al., 2009). We found that a significant proportion of these genes are involved in biological processes related to “cell morphogenesis” (Table S2).

To validate miR-511-3p predicted targets, we first generated a mutant miR-511-3p sequence by substituting four nucleotides in the pre-miR-511 sequence of the SFFV.miR-511 LV. Three out of four substitutions are located in the seed sequence of miR-511-3p, and were selected to not modify the complementary miR-511-5p sequence and to not perturb the stem-loop structure of the pre-miRNA (Figure S3A). We termed the resultant vector SFFV.miR-511-mut LV. To validate the mutant sequence, we transduced RAW264.7 monocytic cells with the miRT-511-5p or -3p reporter LV, and superinfected the transduced cells with the SFFV.miR-511 or -511-mut LV. As shown in Figure 4A, the four mutated nucleotides in the miR-511-3p sequence completely abrogated its activity.

We then performed dual-luciferase assays to test the 3' UTRs of a small panel of miR-511-3p predicted targets, including Rho-dependent kinase-2 (*Rock2*), a serine/threonine kinase that regulates cell's cytoskeleton contractility (Samuel et al., 2011). We first transduced RAW264.7 cells with either SFFV.miR-511 or SFFV.miR-511-mut LV and, 1 week later, transfected the dual-luciferase constructs in the transduced cells. We observed robust *Rock2*-UTR-dependent repression of luciferase activity in SFFV.miR-511-overexpressing cells, but not SFFV.miR-511-mut-overexpressing cells (Figure 4B). We further validated miR-511-3p/*Rock2*-UTR interaction by testing the *Rock2* 3' UTR (as well as a mutated sequence; Figure S3B) in an in vitro GFP repression assay based on our LV reporter system (Figure 4C; Extended Experimental Procedures). By this approach, we confirmed direct interaction between miR-511-3p and the *Rock2* 3' UTR.

Finally, we analyzed the expression of ROCK2 in RAW264.7 cells, P388D1 cells, and BMDMs engineered to overexpress either miR-511 or miR-511-mut. miR-511-3p downregulated ROCK2 both at the mRNA (Figures 4D and 4F) and protein

(E) qPCR of selected miRNAs in MRC1⁺ and CD11c⁺ adipose tissue macrophages isolated from FVB/n mice. The data show relative abundance of each miRNA (mean values ±SEM versus Let7a; n = 3 biological samples). Statistical analysis of the data was performed on ΔC_t values by unpaired Student's t test.

(F) qPCR of selected mRNAs in the adipose tissue macrophages. The data show fold change ($= 2^{\Delta\Delta C_t}$; mean values ±SEM; n = 3 biological samples) versus CD11c⁺ macrophages (reference population). Normalization was performed by $\beta 2 m$. Note that *Tie2* was undetectable in CD11c⁺ macrophages. Statistical analysis of ΔC_t values was performed by unpaired Student's t test.

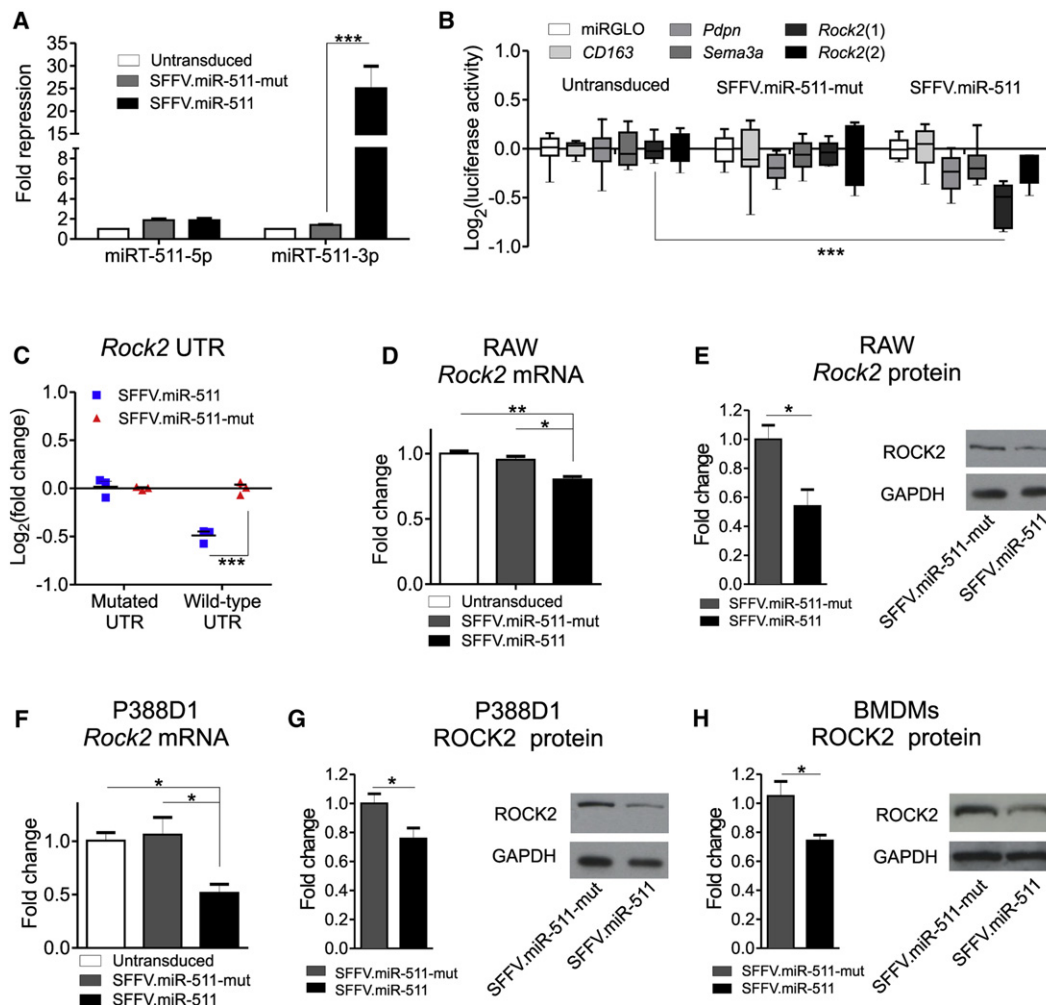


Figure 4. ROCK2 Is a Direct Target of Mouse miR-511-3p

(A) GFP repression in RAW264.7 cells transduced with the miRT-511-5p or -3p LVs and superinfected with the miR-511 or -511-mut overexpressing LVs (mean values \pm SEM versus untransduced [UT] cells; n = 3 independent experiments). Statistical analysis of fold-repression values was performed by two-way ANOVA with Bonferroni posttest.

(B) Firefly luciferase activity in 293T cells untransduced or transduced with either miR-511 or -511-mut LV. The 3' UTRs of mouse podoplanin (*Pdpr*), semaphorin-3A (*Sema3a*), *Rock2* (all miR-511-3p target genes), and *CD163* were tested, together with a UTR-less plasmid (miRGLO). The *Rock2* UTR was split into two fragments (*Rock2*(1) and *Rock2*(2)). The box-and-whisker graph shows luciferase activity (median \pm minimum/maximum values versus miRGLO; n = 6–9 technical replicates from 3 independent experiments). Statistical analysis was performed by two-way ANOVA with Bonferroni posttest.

(C) GFP repression in P388D1 cells transduced with GFP reporter LVs containing either wild-type or mutant UTR sequences from the *Rock2* gene. Cells were superinfected with either miR-511 or -511-mut overexpressing LV. Data show fold change of GFP repression (mean \pm SEM; n = 3 independent experiments). Statistical analysis was performed by two-way ANOVA with Bonferroni posttest.

(D) qPCR of *Rock2* expression in RAW264.7 cells overexpressing either miR-511 or -511-mut. The data show fold change ($= 2^{\Delta\Delta Ct}$; mean values \pm SEM; n = 3 biological samples) versus untransduced cells (reference population). Normalization was performed by $\beta 2 m$. Statistical analysis was performed on actual ΔCt values by unpaired Student's t test.

(E) Western blot analysis of ROCK2 in RAW264.7 cells either overexpressing miR-511 or -511-mut. The left histograms show quantification of ROCK2/GAPDH signal (normalized to miR-511-mut; seven technical replicates from three independent experiments). Statistical analysis was performed by paired Student's t test. A representative blot is shown on the right.

(F) qPCR of *Rock2* expression in P388D1 cells overexpressing either miR-511 or -511-mut. The data show fold change ($= 2^{\Delta\Delta Ct}$; mean values \pm SEM; n = 3 biological samples) versus untransduced cells (reference population). Normalization was performed by *Hprt*. Statistical analysis of ΔCt values was performed by unpaired Student's t test.

(G and H) Western blot analysis of ROCK2 in P388D1 cells (G) or BMDMs (H) overexpressing either miR-511 or -511-mut. Analysis as in (E) (P388D1: nine technical replicates, three independent experiments; BMDMs: four technical replicates, two independent experiments).

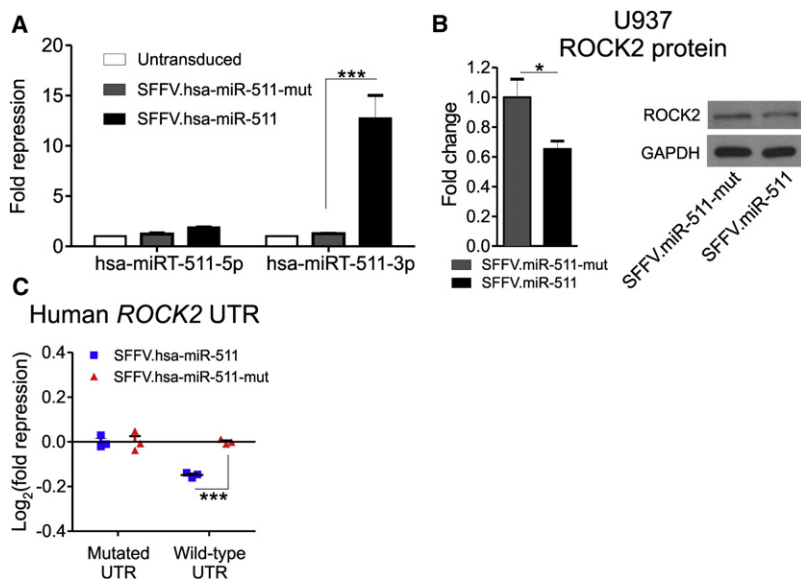


Figure 5. ROCK2 Is a Direct Target of Human miR-511-3p

(A) miR-511-3p and -5p activity in U937 cells overexpressing either miR-511 or -511-mut. The histogram shows GFP repression (mean values \pm SEM versus untransduced cells; $n = 3$ independent experiments). Statistical analysis of fold-repression values was performed by two-way ANOVA with Bonferroni posttest.

(B) Western blot analysis of ROCK2 in U937 cells overexpressing either miR-511 or -511-mut. The left histograms show quantification of ROCK2/GAPDH signal (normalized to miR-511-mut; nine technical replicates from three independent experiments). Statistical analysis was performed by paired Student's *t* test. A representative blot is shown on the right.

(C) GFP repression in U937 cells transduced with GFP reporter LVs containing either wild-type or mutant UTR sequences from the *ROCK2* gene. Cells were superinfected with either miR-511 or -511-mut overexpressing LV. Data show fold change of GFP repression (mean \pm SEM; $n = 3$ independent experiments). Statistical analysis was performed by two-way ANOVA with Bonferroni posttest.

(Figures 4E, 4G, and 4H) level. Taken together, these data demonstrate that ROCK2 is a direct target of mouse miR-511-3p.

The Human *MRC1* Gene Encodes for an Active miR-511-3p Sequence

The human *MRC1* gene contains a miR-511 sequence (hsa-miR-511) located in the fifth intron of the gene; of note, hsa-miR-511-3p is a miRNA, currently not annotated in miRBase (<http://www.mirbase.org>). The mature hsa-miR-511-3p but not -5p sequence is conserved in *M. musculus* and *H. sapiens* (Figure S4A). We then asked whether miR-511-3p activity is conserved in the two species. To identify the active strand of the human miR-511, we generated both reporter and overexpressing LVs (Figure S4B), as described above for the mouse miR-511. We transduced human U937 monocytic cells with the reporter LVs and then superinfected the transduced cells with the overexpressing LVs. Analysis of GFP repression showed that, as in the mouse system, miR-511-3p is the active strand of the human pre-miR-511 (Figure 5A).

As in the mouse system, predicted targets of human miR-511-3p (Table S3) comprise genes involved in biological processes related to "cell morphogenesis" (Table S4). Overexpression of human miR-511-3p decreased ROCK2 protein in U937 cells (Figure 5B), suggesting that *ROCK2* is a direct target of human miR-511-3p, as predicted by TargetRank (Nielsen et al., 2007). We confirmed this finding by analyzing human miR-511-3p/*ROCK2*-UTR interaction in an in vitro GFP repression assay based on our reporter LV system (Figure 5C; Extended Experimental Procedures). Together, these data strongly suggest that miR-511-3p activity is conserved in mice and humans.

Overexpression of miR-511-3p in BM-Derived Cells Inhibits Tumor Growth and Alters Tumor Blood Vessel Morphology

To study the biological function of mouse miR-511-3p, we overexpressed it in BM-derived hematopoietic cells. To this aim, we

transduced HS/PCs obtained from CD45.1/C57BL/6 mice with either SFFV.miR-511 or -511-mut LV, and transplanted the transduced cells into irradiated, congenic CD45.2/C57BL/6 mice, to obtain SFFV.miR-511 and SFFV.miR-511-mut mice, respectively. Four weeks after the transplant, we inoculated LLC cells subcutaneously in the transplanted mice and monitored tumor growth for 3–4 weeks.

Unexpectedly, miR-511-3p overexpression in hematopoietic cells inhibited LLC growth (Figure 6A). We could reasonably exclude that tumor growth inhibition by miR-511-3p overexpression was due to defective hematopoiesis and/or altered recruitment of hematopoietic cells to the tumors. Indeed, miR-511-3p overexpression in hematopoietic cells did not affect the repopulating activity of the transduced HS/PCs, as shown by the similarly high frequency of CD45.1⁺OFP⁺, donor-transduced hematopoietic cells in the blood of both groups of mice (Figure S5A). Furthermore, miR-511-3p overexpression neither affected the recruitment of F4/80⁺ TAMs (which represent up to 60% of all tumor-infiltrating hematopoietic cells in this tumor model), Gr1⁺ neutrophils, NK, T and B cells to the tumors (Figure S5B), nor the relative frequency of MRC1⁺ and CD11c⁺ TAM subsets (Figure S5C).

We then asked whether miR-511-3p overexpression influenced tumor angiogenesis. Although we did not observe changes in vascular density by immunofluorescence staining of tumor sections (data not shown), we noted that miR-511-3p overexpression altered the architecture of the tumor microvascular network by augmenting blood vessel tortuosity and the occurrence of enlarged, glomerular-like structures (Figures 6B and 6C). Accordingly, morphometric analysis of thick tumor sections showed similar vascular area but significantly reduced total and mean length of blood vessels in SFFV.miR-511 compared with -511-mut mice (Figure 6D). Together, these data indicate that miR-511-3p overexpression in BM-derived cells inhibits tumor growth and dysregulates angiogenesis without affecting hematopoiesis detectably.

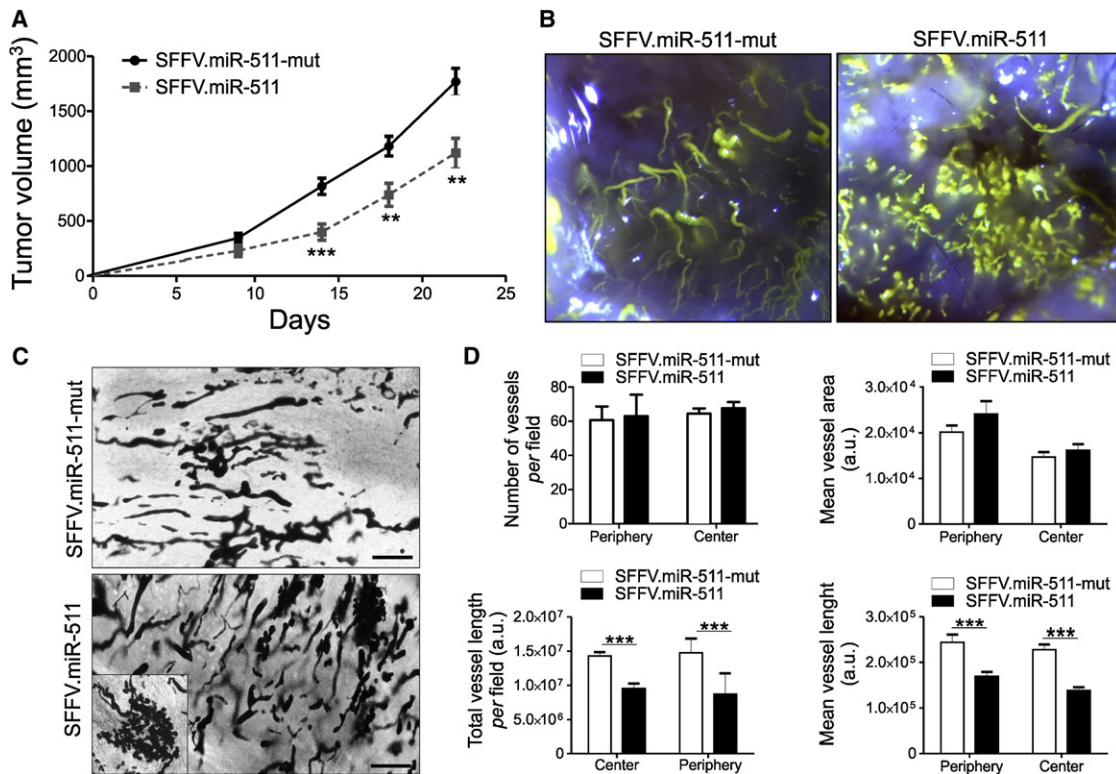


Figure 6. miR-511-3p Overexpression in TAMs Inhibits Tumor Growth and Alters Blood Vessel Morphology

(A) LLC growth in mice overexpressing either miR-511 or -511-mut in hematopoietic cells. Data show tumor volumes (mean values \pm SEM; $n = 11$ mice/group). Statistical analysis was performed by unpaired Student's *t* test. One representative experiment of two performed is shown.

(B) Whole-mount visualization of blood vessels by Microfill perfusion. LLCs ($n = 5$ /group) were grown in mice overexpressing either miR-511 or -511-mut in hematopoietic cells.

(C) Representative 200- μ m-thick tumor sections (of eight sections/tumor and $n = 5$ tumors/group). The inset in the bottom panel shows blood vessels with glomerular morphology. Scale bar, 200 μ m.

(D) Morphometric analysis of blood vessels in LLCs ($n = 5$ /group) grown in mice overexpressing either miR-511 or -511-mut in hematopoietic cells. Data were obtained by analyzing eight sections/tumor (four from the tumor periphery and four from the central tumor mass) and $n = 5$ tumors/group. Data are expressed as arbitrary units. Statistical analysis was performed by unpaired Student's *t* test.

Overexpression of miR-511-3p in TAMs Globally Downregulates miR-511-3p Predicted Target Genes

Because the genetic programs of TAMs may influence tumor angiogenesis and growth (Qian and Pollard, 2010), we asked whether miR-511-3p overexpression had modulated TAM's gene expression. To address this question, we sorted F4/80⁺OPP⁺ TAMs from LLCs grown in SFFV.miR-511 or -511-mut mice. qPCR analysis of selected miRNAs showed that the SFFV.miR-511 LV upregulated the expression of miR-511-3p by \sim 5-fold in the F4/80⁺OPP⁺ TAMs of SFFV.miR-511 compared to -511-mut mice, which only express the endogenous miR-511-3p sequence (Figure 7A). Of note, miR-511-3p-mut was only detected in the TAMs of SFFV.miR-511-mut mice, whereas miR-511-5p was expressed by both SFFV.miR-511 and SFFV.miR-511-mut TAMs. However, as seen in the TAMs of MMTV-PyMT mice (Figure 2D), expression of miR-511-5p was much lower than miR-511-3p, strongly suggesting that, even when overexpressed, it is rapidly degraded *in vivo*.

We then performed RNA-Seq analyses of the transcriptome of sorted F4/80⁺OPP⁺ TAMs. We used the Illumina HiSeq 2000 platform and retrieved 249 genes (out of 16,355; 1.5%;

$p < 0.05$ adjusted for false discovery rate) that were differentially expressed in the TAMs of SFFV.miR-511 versus -511-mut mice (Table S5). Remarkably, it was found that the predicted targets of miR-511-3p (Table S1) were globally downregulated by miR-511-3p overexpression in TAMs (Figure 7B). We also used TargetRank to identify transcripts that contain in their 3' UTR at least one sequence with perfect complementarity to the seed sequence of miR-511-3p (i.e., M8-A1 8-mer and M8 7-mer binding sites; Table S6), and found that such transcripts were globally downregulated by miR-511-3p overexpression (Figure 7C; see Extended Experimental Procedures). Conversely, genes containing M8-A1 8-mer or M8 7-mer binding sites for either miR-511-5p or -3p-mut were significantly less downregulated by miRNA overexpression (Figures 7D and 7E). These data demonstrate broad and robust miR-511-3p activity in TAMs by our overexpression platform.

Overexpression of miR-511-3p Tunes down the Protumoral Gene Signature of MRC1⁺ TAMs

Although the vast majority of the differentially expressed genes were downregulated by miR-511-3p overexpression in TAMs

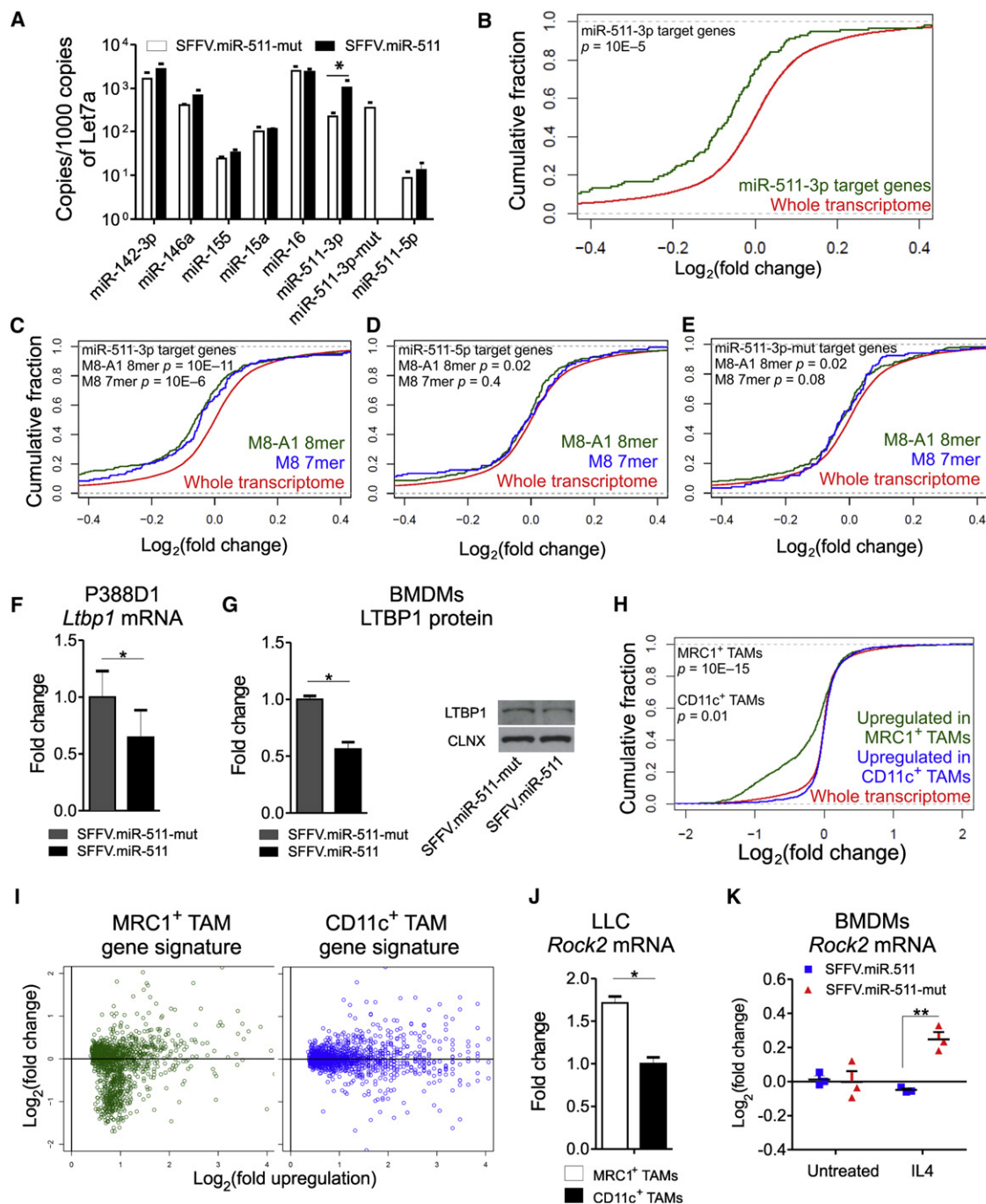


Figure 7. miR-511-3p Overexpression in TAMs Tunes Down Their Protumoral Gene Signature

(A) qPCR of selected miRNAs in F4/80⁺OPF⁺ TAMs isolated from LLCs grown in mice overexpressing either miR-511 or -511-mut in hematopoietic cells. The data show the relative abundance of each miRNA (mean values ± SEM versus Let7a; n = 4 biological samples). Statistical analysis of ΔC_t values was performed by unpaired Student's t test.

(B) Cumulative distribution of fold changes in the whole transcriptome (13,747 genes; transcripts with less than 10 reads, and miR-511-3p predicted targets were excluded from the analysis) of TAMs overexpressing miR-511 (versus -511-mut; red line). The green line shows the cumulative distribution of fold changes in transcripts that are miR-511-3p predicted targets (145 genes). Note the global repression of miR-511-3p target genes. Statistical analysis was performed by one-sided Kolmogorov-Smirnov test.

(C–E) Cumulative distribution of fold changes in the whole transcriptome (13,747 genes; transcripts with less than 10 reads, and miR-511-3p predicted targets were excluded) of TAMs overexpressing miR-511 (versus -511-mut; red line). The green and blue lines show the cumulative distribution of fold changes in transcripts that contain M8-A1 8-mer and M8 7-mer target sites, respectively, for miR-511-3p (C), -5p (D), or -3p-mut (E). Statistical analysis was performed by one-sided Kolmogorov-Smirnov test.

(Table S5), they could not be identified as miR-511-3p direct targets by TargetScan, DIANA microT, and TargetRank, and possibly represent indirect targets of the miRNA. Interestingly, the downregulated genes are primarily involved in biological processes related to cell adhesion, morphogenesis, and ECM organization (Table S7). They comprise genes encoding for ECM proteins, such as collagens (e.g., type VI collagens), basal lamina proteins, and proteoglycans. Downregulated genes also include genes that control the synthesis and remodeling of the ECM, such as proteases (e.g., *Adamst1*, *Adamst11*, *Mmp11*, *Mmp3*), scavenger receptors (e.g., *Sparc* and *Mrc2*), and TGF- β family (e.g., *Tgfb3*, *Bmp1*, *Bmpr1a*) or associated (*Ltbp1*) factors. Latent TGF- β binding protein-1 (LTBP1) is a secreted protein that has a role in the assembly, secretion, and activation of latent complexes of TGF- β in the ECM; by activating TGF- β , LTBP1 may stimulate ECM biosynthesis and enhance tumor growth (Saunier and Akhurst, 2006). Consistent with RNA-Seq analysis of TAMs (Table S5), miR-511-3p overexpression in P388D1 cells and BMDMs decreased expression of LTBP1 at the mRNA (Figure 7F) and protein (Figure 7G) level, respectively.

We and others previously showed that MRC1⁺ TAMs express a distinguishing gene signature and are protumoral in mouse models of cancer; genes upregulated in MRC1⁺ TAMs may thus identify the protumoral gene signature of TAMs (Pucci et al., 2009; Movahedi et al., 2010). We then hypothesized that miR-511-3p overexpression inhibited tumor growth by attenuating the protumoral genetic programs of MRC1⁺ TAMs. To test this hypothesis, we first sorted MRC1⁺ and CD11c⁺ TAMs from LLC tumors grown for 4 weeks in wild-type, nontransplanted C57BL/6 mice, and subjected the isolated cells to RNA-Seq analysis. About 14% of the identified genes were differentially expressed between MRC1⁺ and CD11c⁺ TAMs ($p < 0.05$ adjusted for false discovery rate; Table S8), corroborating the notion that MRC1⁺ and CD11c⁺ TAMs represent distinct cell subsets (Pucci et al., 2009). Of note, many of the genes upregulated in MRC1⁺ versus CD11c⁺ TAMs encode for molecules with previously established protumoral bioeffector function (Table S8; Pucci et al., 2009). We then analyzed the effects of miR-511-3p overexpression on the genes specifically upregulated in either MRC1⁺ or CD11c⁺ TAMs. Interestingly,

miR-511-3p overexpression in TAMs tuned down the expression of a significant proportion of the genes upregulated in MRC1⁺ TAMs, whereas it did not modulate genes upregulated in CD11c⁺ TAMs (Figures 7H and 7I; Table S9). These data imply that miR-511-3p may function as a negative regulator of TAM's protumoral genetic programs.

Although RNA-Seq profiling did not detect statistically significant upregulation of *Rock2* in MRC1⁺ versus CD11c⁺ TAMs (while showing a clear trend toward statistical significance), qPCR analyses consistently showed higher *Rock2* expression in MRC1⁺ than CD11c⁺ TAMs (Figure 7J). We, therefore, used *Rock2* as a model gene representative of the MRC1⁺ TAM signature, and asked whether miR-511-3p could attenuate its upregulation in MRC1⁺ macrophages. We measured *Rock2* mRNA by qPCR in BMDMs that overexpressed either SFFV.miR-511 or SFFV.miR-511-mut and that were cultured in the presence of IL-4 or left untreated. Consistent with our predictions, IL-4 upregulated *Rock2* in BMDMs, but this effect was abrogated by miR-511-3p overexpression (Figure 7K). Because IL-4-stimulated BMDMs may model protumoral TAMs in vitro (Biswas and Mantovani, 2010), these data provide proof of concept that miR-511-3p may function as a negative regulator of protumoral gene expression in MRC1⁺ macrophages.

DISCUSSION

In this study we show that upregulation of the mannose receptor, MRC1, in both tissue-resident and tumor macrophages is accompanied by an increase of a previously uncharacterized miRNA, miR-511-3p. The bioactivity of miR-511-3p correlates with the magnitude of MRC1 expression in both tissue-resident and tumor macrophages, suggesting that *Mrc1* and miR-511-3p are transcriptionally coregulated. By employing a genetic strategy to stably overexpress miRNAs in BM-derived cells, we found that miR-511-3p broadly and specifically attenuates the expression of genes that define the protumoral signature of MRC1⁺ TAMs (Pucci et al., 2009; Movahedi et al., 2010). Consistent with this finding, miR-511-3p overexpression inhibited tumor growth. On the other hand, miR-511-3p overexpression did not alter the proinflammatory gene signature of CD11c⁺

(F) qPCR of *Ltbp1* expression in P388D1 cells overexpressing either miR-511 or -511-mut. The data show fold change ($= 2^{\Delta Ct}$; mean values \pm SEM; $n = 3$ biological samples) versus miR-511-3p-mut (reference population). Normalization was performed by *Hprt*. Statistical analysis of ΔCt values was performed by unpaired Student's *t* test.

(G) Western blot analysis of LTBP1 in BMDMs either overexpressing mouse miR-511 or -511-mut. The left histograms show quantification of LTBP1/calnexin (CLNX) signal (normalized to miR-511-mut; four technical replicates from two independent experiments). Statistical analysis was performed by paired Student's *t* test. A representative blot is shown on the right.

(H) Cumulative distribution of fold changes in the whole transcriptome (16,355 genes) of TAMs overexpressing miR-511 (versus -511-mut; red line). The green line shows the cumulative distribution of fold changes in transcripts that are upregulated in MRC1⁺ TAMs (versus CD11c⁺ TAMs; 1,365 genes); The blue line shows the cumulative distribution of fold changes in the transcripts that are upregulated in CD11c⁺ TAMs (versus MRC1⁺ TAMs; 1,596 genes). Statistical analysis was performed by one-sided Kolmogorov-Smirnov test.

(I) Scatterplot distribution of fold changes in gene expression of MRC1⁺ and CD11c⁺ TAMs overexpressing miR-511 (versus -511-mut). The x axis shows the upregulation of transcripts in MRC1⁺ versus CD11c⁺ TAMs (left; MRC1⁺ TAM gene signature) or CD11c⁺ versus MRC1⁺ TAMs; (right; CD11c⁺ TAM gene signature). The y axis shows changes in gene expression by miR-511 overexpression (versus -511-mut). Transcripts with less than ten reads were excluded from the analysis. Statistical analysis of the data is presented in (H).

(J) qPCR of *Rock2* expression in MRC1⁺ and CD11c⁺ TAMs isolated from LLCs. The data show fold change ($= 2^{\Delta Ct}$; mean values \pm SEM; $n = 2$ biological samples) versus CD11c⁺ TAMs (reference population). Normalization was performed by $\beta 2m$. Statistical analysis of ΔCt values was performed by unpaired Student's *t* test.

(K) qPCR of *Rock2* expression in BMDMs either untreated or stimulated by IL-4; the cells were transduced with either miR-511 or -511-mut overexpressing LV. Data show fold change in *Rock2* repression (mean \pm SEM; $n = 3$ independent experiments) versus untreated cells. Note that miR-511 overexpression abrogates IL-4-induced *Rock2* upregulation in the cells. Statistical analysis was performed by two-way ANOVA with Bonferroni posttest.

macrophages (Pucci et al., 2009; Movahedi et al., 2010), suggesting specific activity of the miRNA in a TAM subtype. Interestingly, miR-511-3p was most biologically active in tissue-resident macrophages bearing features of AAMs (Chawla et al., 2011; Gordon and Martinez, 2010; Landsman and Jung, 2007; Martinez et al., 2009). These cells are known to participate in both pathological and physiological processes, including host defense from parasites, stimulation of angiogenesis and tissue repair, promotion of tissue fibrosis, and regulation of organ metabolism (Gordon and Martinez, 2010). Future studies are now needed to address the significance of miR-511-3p in the regulation of alternative activation of macrophages.

Interestingly, miR-511-3p downregulated TAM expression of multiple genes involved in ECM synthesis and remodeling; these include collagens and other fibrous proteins, proteases, and scavenger receptors. Of note, the composition and biophysical properties of the ECM influence tumor growth and progression. Increased collagen deposition/crosslinking and ECM stiffening stimulate tumor cell proliferation, invasion, and malignancy (Egeblad et al., 2010; Levental et al., 2009). Furthermore, the composition and biophysical properties of the ECM regulate vascular morphogenesis in tumors (Bauer et al., 2009). Indeed, ECM density controls the extension speed of vascular sprouts, and a high matrix-fiber anisotropy (i.e., directional tension) provides strong contact guidance cues for endothelial cells and stimulates sprout branching (Bauer et al., 2009). Although ECM fibrous proteins are mainly produced by fibroblasts and epithelial cells (Egeblad et al., 2010; Kalluri and Zeisberg, 2006), there is also evidence that some collagens and other ECM proteins may be robustly expressed by in vitro-cultured macrophages (Schnoor et al., 2008). Yet, the significance of TAM-produced ECM fibrous proteins for tumor growth and vascularization has remained largely unexplored. Our deep sequencing analyses indicate that MRC1⁺ TAMs express several ECM genes (including genes encoding for collagens and other fibrous proteins), which were globally and significantly downregulated by miR-511-3p overexpression in TAMs. Because MRC1⁺ TAMs represent a major component of the perivascular tumor stroma and support vascular morphogenesis in tumors (Mazzieri et al., 2011; Squadrito and De Palma, 2011), modulation of ECM-protein synthesis/remodeling by miR-511-3p in MRC1⁺ TAMs may have the potential to influence ECM dynamics in the perivascular microenvironment. This would be consistent with our finding that miR-511-3p overexpression in TAMs altered the morphology of intratumoral blood vessels, possibly as a consequence of changes in the biophysical properties of the perivascular ECM (and/or in the levels of TAM-derived angiogenic factors). It is also possible that miR-511-3p is horizontally transferred from MRC1⁺ TAMs to other tumor-associated stromal cells via microvesicles or exosomes (Yang et al., 2011).

We identified ROCK2 as a direct target of miR-511-3p. Our data indicate that MRC1⁺ TAMs as well as IL-4-polarized BMDMs express higher *Rock2* mRNA levels than CD11c⁺MRC1⁻ TAMs or unstimulated BMDMs. Of note, constitutive ROCK activation in epidermal cells increases collagen synthesis and tissue stiffness (Samuel et al., 2011). It is tempting to speculate that increased ROCK activity in MRC1⁺ TAMs might

enhance their expression and secretion of ECM proteins as part of their protumoral genetic program. Because miR-511-3p downregulated ROCK2 both at the mRNA and protein level, our data suggest that miR-511-3p might negatively regulate ROCK activity in MRC1⁺ TAMs and downregulate their expression of ECM genes relevant to tumor progression.

Although several miRNAs have been identified that regulate immune cell functions (O'Connell et al., 2010), little is known of their roles in the modulation of TAM heterogeneity and functions. A recent report used Illumina miRNA Chips to analyze the miRNA expression signature of human monocytes and monocyte-derived DCs/macrophages (Tserel et al., 2011). Several miRNAs were found to be differentially expressed between DCs/macrophages and freshly isolated monocytes. Among these, human miR-511 (representing the hsa-miR-511-5p sequence described in our study) was highly upregulated in DCs/macrophages (Tserel et al., 2011). Although the report of Tserel and colleagues may appear consistent with our findings, we did not detect significant activity of either human or mouse miR-511-5p in several independent cell assays, both in vitro and in vivo. Conversely, we identified miR-511-3p as the bioactive strand of both human and mouse pre-miR-511. It should be noted, however, that the human miR-511-3p sequence is not annotated in miRBase and was not assayed in the Illumina miRNA Chips employed by Tserel and colleagues, so its differential expression could not be assessed (Tserel et al., 2011). Although the mechanisms that regulate miRNA strand selection are still unclear, it is likely that the thermodynamic stability of the two ends of the pre-miRNA determines which strand is to be selected for loading into the RISC complex, and which is to be degraded (Khvorova et al., 2003). Recent studies have also illustrated that miRNA strand selection may be cell type, context, and species specific (Biasiolo et al., 2011; Kuchenbauer et al., 2011). Nevertheless, our analyses indicate that miR-511-3p but not -5p is highly conserved across mammalian species, pointing to a preeminent role of this miRNA strand. Further studies are, therefore, needed to clarify the significance of miR-511-5p expression and activity in macrophages.

In summary our findings reveal an unexpected layer of gene expression control in TAMs, which relies on an endogenous molecular switch that is activated in a tumor-promoting (MRC1⁺) subset of these cells. Enhancing miR-511-3p activity in TAMs (e.g., via delivery of macrophage-targeted miRNA carriers) may represent a therapeutic strategy to reprogram them from a protumoral to an antitumoral phenotype.

EXPERIMENTAL PROCEDURES

Detailed experimental procedures are presented as [Extended Experimental Procedures](#).

Mice

C57BL/6, CD45.1/C57BL/6, and FVB/n mice were purchased by Charles River Laboratory (Calco, Milan). FVB/MMTV-PyMT mice were obtained from the NCI-Frederick Mouse Repository (Frederick, MD) and established as a colony at the San Raffaele animal facility. All procedures were performed according to protocols approved by the Animal Care and Use Committee of the Fondazione San Raffaele del Monte Tabor (IACUC 324, 335, and 447) and communicated to the Ministry of Health and local authorities according to the Italian law.

LV Transduction

For experiments in vitro, cells were transduced with LV doses ranging from 10^4 to 10^5 transducing units (TU)/ml. When required, sequential transduction was performed by (i) transducing the cells with the first LV; (ii) washing and replating the cells; and (iii) transducing the cells with the second LV (superinfection) on day 5–7 after the first transduction. For HS/PC transplantation, 10^6 HS/PCs/ml were prestimulated for 6 hr in serum-free medium containing a cocktail of cytokines, and then transduced with miRT reporter or miR-511-overexpressing LVs with a dose equivalent to 10^8 TU/ml. After transduction, 10^6 cells were infused into the tail vein of lethally irradiated mice

Tumor Experiments

LLC/3LL cells (5×10^6) were injected subcutaneously in syngenic C57BL/6 mice, and tumors were grown for 3–4 weeks; tumor size was determined by caliper measurements. N202 mammary carcinoma cells (5×10^6) were injected subcutaneously in syngenic FVB/n mice, and tumors were grown for 4 weeks.

For miRT reporter studies we performed two independent experiments. In the first experiment, transduced HS/PCs were transplanted in irradiated C57BL/6 mice, which were subsequently challenged with LLC cells. In the second experiment, transduced HS/PCs were transplanted in irradiated FVB/n mice, subsequently challenged with N202 cells. For miR overexpression studies we performed three independent experiments. In each experiment, transduced HS/PCs were transplanted in irradiated C57BL/6 mice, subsequently challenged with LLC cells; tumor growth was analyzed for 3–4 weeks in the first two experiments. In the first experiment, tumors were also harvested for sorting of TAMs and RNA-Seq analysis. In the second experiment, mice were randomly selected for Microfill perfusion and analysis of the tumor-associated vasculature. In the third experiment, tumors were harvested for sorting of TAMs and qPCR of miRNAs.

Calculation of miRNA Activity

In most of the experiments, we calculated miR-511-mediated GFP repression (indicated as “fold-repression”) in live cells by using the following equation:

$$\left[\text{MFI } \Delta\text{LNGFR}_{\text{miRT}} \times (\text{MFI GFP}_{\text{miRT}})^{-1} \right] / \left[\text{MFI } \Delta\text{LNGFR}_{\text{no-miRT}} \times (\text{MFI GFP}_{\text{no-miRT}})^{-1} \right],$$

where MFI is the *mean fluorescence activity* of either GFP or ΔLNGFR measured by flow cytometry.

Statistical Analysis

Statistical analysis of the data is described in the figure legends and [Extended Experimental Procedures](#). Statistical significance of the data is indicated as follows: *; $p < 0.05$; **; $p < 0.01$; ***; $p < 0.001$.

ACCESSION NUMBERS

RNA sequencing data (12 TAM samples) have been deposited in the GEO repository at NCBI under accession number GSE34903.

SUPPLEMENTAL INFORMATION

Supplemental Information includes five figures, 13 tables, and [Extended Experimental Procedures](#) and can be found with this article online at doi:10.1016/j.celrep.2011.12.005.

LICENSING INFORMATION

This is an open-access article distributed under the terms of the Creative Commons Attribution-Noncommercial-No Derivative Works 3.0 Unported License (CC-BY-NC-ND; <http://creativecommons.org/licenses/by-nc-nd/3.0/legalcode>).

ACKNOWLEDGMENTS

We thank Emanuele Canonico for cell sorting and Alberto Gallotti for help with some experiments. This research was supported by the European Research Council (Starting Grant 243128/TIE2+Monocytes to M.D.P.) and Associazione Italiana per la Ricerca sul Cancro (AIRC IG-2010 to M.D.P.; AIRC IG-2010 to L.N.). F.P. was supported by a Fondazione Italiana per la Ricerca sul Cancro (FIRC) fellowship.

Received: August 8, 2011

Revised: December 15, 2011

Accepted: December 19, 2011

Published online: February 9, 2012

REFERENCES

- Bartel, D.P. (2009). MicroRNAs: target recognition and regulatory functions. *Cell* 136, 215–233.
- Baskerville, S., and Bartel, D.P. (2005). Microarray profiling of microRNAs reveals frequent coexpression with neighboring miRNAs and host genes. *RNA* 11, 241–247.
- Bauer, A.L., Jackson, T.L., and Jiang, Y. (2009). Topography of extracellular matrix mediates vascular morphogenesis and migration speeds in angiogenesis. *PLoS Comput. Biol.* 5, e1000445.
- Biasiolo, M., Sales, G., Lionetti, M., Agnelli, L., Todoerti, K., Bisognin, A., Coppe, A., Romualdi, C., Neri, A., and Bortoluzzi, S. (2011). Impact of host genes and strand selection on miRNA and miRNA* expression. *PLoS One* 6, e23854.
- Biswas, S.K., and Mantovani, A. (2010). Macrophage plasticity and interaction with lymphocyte subsets: cancer as a paradigm. *Nat. Immunol.* 11, 889–896.
- Brown, B.D., Gentner, B., Cantore, A., Colleoni, S., Amendola, M., Zingale, A., Baccarini, A., Lazzari, G., Galli, C., and Naldini, L. (2007). Endogenous microRNA can be broadly exploited to regulate transgene expression according to tissue, lineage and differentiation state. *Nat. Biotechnol.* 25, 1457–1467.
- Chawla, A., Nguyen, K.D., and Goh, Y.P. (2011). Macrophage-mediated inflammation in metabolic disease. *Nat. Rev. Immunol.* 11, 738–749.
- DeNardo, D.G., Andreu, P., and Coussens, L.M. (2010). Interactions between lymphocytes and myeloid cells regulate pro- versus anti-tumor immunity. *Cancer Metastasis Rev.* 29, 309–316.
- De Palma, M., Venneri, M.A., Galli, R., Sergi Sergi, L., Politi, L.S., Sampaoli, M., and Naldini, L. (2005). Tie2 identifies a hematopoietic lineage of proangiogenic monocytes required for tumor vessel formation and a mesenchymal population of pericyte progenitors. *Cancer Cell* 8, 211–226.
- Egeblad, M., Rasch, M.G., and Weaver, V.M. (2010). Dynamic interplay between the collagen scaffold and tumor evolution. *Curr. Opin. Cell Biol.* 22, 697–706.
- Gordon, S., and Martinez, F.O. (2010). Alternative activation of macrophages: mechanism and functions. *Immunity* 32, 593–604.
- Huang, D.W., Sherman, B.T., and Lempicki, R.A. (2009). Systematic and integrative analysis of large gene lists using DAVID bioinformatics resources. *Nat. Protoc.* 4, 44–57.
- Kalluri, R., and Zeisberg, M. (2006). Fibroblasts in cancer. *Nat. Rev. Cancer* 6, 392–401.
- Khvorova, A., Reynolds, A., and Jayasena, S.D. (2003). Functional siRNAs and miRNAs exhibit strand bias. *Cell* 115, 209–216.
- Kuchenbauer, F., Mah, S.M., Heuser, M., McPherson, A., Rüschemann, J., Rouhi, A., Berg, T., Bullinger, L., Argiropoulos, B., Morin, R.D., et al. (2011). Comprehensive analysis of mammalian miRNA* species and their role in myeloid cells. *Blood* 118, 3350–3358.
- Landsman, L., and Jung, S. (2007). Lung macrophages serve as obligatory intermediate between blood monocytes and alveolar macrophages. *J. Immunol.* 179, 3488–3494.

- Levental, K.R., Yu, H., Kass, L., Lakins, J.N., Egeblad, M., Erler, J.T., Fong, S.F., Csiszar, K., Giaccia, A., Weninger, W., et al. (2009). Matrix crosslinking forces tumor progression by enhancing integrin signaling. *Cell* **139**, 891–906.
- Lewis, B.P., Burge, C.B., and Bartel, D.P. (2005). Conserved seed pairing, often flanked by adenosines, indicates that thousands of human genes are microRNA targets. *Cell* **120**, 15–20.
- Maragkakis, M., Alexiou, P., Papadopoulos, G.L., Reczko, M., Dalamagas, T., Giannopoulos, G., Goumas, G., Koukis, E., Kourtis, K., Simossis, V.A., et al. (2009). Accurate microRNA target prediction correlates with protein repression levels. *BMC Bioinformatics* **10**, 295.
- Martinez, F.O., Helming, L., and Gordon, S. (2009). Alternative activation of macrophages: an immunologic functional perspective. *Annu. Rev. Immunol.* **27**, 451–483.
- Mazzieri, R., Pucci, F., Moi, D., Zonari, E., Ranghetti, A., Berti, A., Politi, L.S., Gentner, B., Brown, J.L., Naldini, L., and De Palma, M. (2011). Targeting the ANG2/TIE2 axis inhibits tumor growth and metastasis by impairing angiogenesis and disabling rebounds of proangiogenic myeloid cells. *Cancer Cell* **19**, 512–526.
- Movahedi, K., Laoui, D., Gysemans, C., Baeten, M., Stangé, G., Van den Bosche, J., Mack, M., Pipeleers, D., In't Veld, P., De Baetselier, P., and Van Ginnecht, J.A. (2010). Different tumor microenvironments contain functionally distinct subsets of macrophages derived from Ly6C(high) monocytes. *Cancer Res.* **70**, 5728–5739.
- Nielsen, C.B., Shomron, N., Sandberg, R., Hornstein, E., Kitzman, J., and Burge, C.B. (2007). Determinants of targeting by endogenous and exogenous microRNAs and siRNAs. *RNA* **13**, 1894–1910.
- O'Connell, R.M., Rao, D.S., Chaudhuri, A.A., and Baltimore, D. (2010). Physiological and pathological roles for microRNAs in the immune system. *Nat. Rev. Immunol.* **10**, 111–122.
- Pucci, F., Venneri, M.A., Biziato, D., Nonis, A., Moi, D., Sica, A., Di Serio, C., Naldini, L., and De Palma, M. (2009). A distinguishing gene signature shared by tumor-infiltrating Tie2-expressing monocytes, blood “resident” monocytes, and embryonic macrophages suggests common functions and developmental relationships. *Blood* **114**, 901–914.
- Qian, B.Z., and Pollard, J.W. (2010). Macrophage diversity enhances tumor progression and metastasis. *Cell* **141**, 39–51.
- Rolny, C., Mazzone, M., Tugues, S., Laoui, D., Johansson, I., Coulon, C., Squadrito, M.L., Segura, I., Li, X., Knevels, E., et al. (2011). HRG inhibits tumor growth and metastasis by inducing macrophage polarization and vessel normalization through downregulation of PlGF. *Cancer Cell* **19**, 31–44.
- Samuel, M.S., Lopez, J.I., McGhee, E.J., Croft, D.R., Strachan, D., Timpson, P., Munro, J., Schröder, E., Zhou, J., Brunton, V.G., et al. (2011). Actomyosin-mediated cellular tension drives increased tissue stiffness and β -catenin activation to induce epidermal hyperplasia and tumor growth. *Cancer Cell* **19**, 776–791.
- Saunier, E.F., and Akhurst, R.J. (2006). TGF beta inhibition for cancer therapy. *Curr. Cancer Drug Targets* **6**, 565–578.
- Schnoor, M., Cullen, P., Lorkowski, J., Stolle, K., Robenek, H., Troyer, D., Rauterberg, J., and Lorkowski, S. (2008). Production of type VI collagen by human macrophages: a new dimension in macrophage functional heterogeneity. *J. Immunol.* **180**, 5707–5719.
- Sica, A., and Bronte, V. (2007). Altered macrophage differentiation and immune dysfunction in tumor development. *J. Clin. Invest.* **117**, 1155–1166.
- Squadrito, M.L., and De Palma, M. (2011). Macrophage regulation of tumor angiogenesis: implications for cancer therapy. *Mol. Aspects Med.* **32**, 123–145.
- Stein, M., Keshav, S., Harris, N., and Gordon, S. (1992). Interleukin 4 potently enhances murine macrophage mannose receptor activity: a marker of alternative immunologic macrophage activation. *J. Exp. Med.* **176**, 287–292.
- Taylor, P.R., Martinez-Pomares, L., Stacey, M., Lin, H.H., Brown, G.D., and Gordon, S. (2005). Macrophage receptors and immune recognition. *Annu. Rev. Immunol.* **23**, 901–944.
- Tserel, L., Runnel, T., Kisand, K., Pihlap, M., Bakhoff, L., Kolde, R., Peterson, H., Vilo, J., Peterson, P., and Rebane, A. (2011). MicroRNA expression profiles of human blood monocyte-derived dendritic cells and macrophages reveal miR-511 as putative positive regulator of Toll-like receptor 4. *J. Biol. Chem.* **286**, 26487–26495.
- Yang, M., Chen, J., Su, F., Yu, B., Su, F., Lin, L., Liu, Y., Huang, J.D., and Song, E. (2011). Microvesicles secreted by macrophages shuttle invasion-potentiating microRNAs into breast cancer cells. *Mol. Cancer* **10**, 117.